Supporting Information for

Improving Diacetylene Photopolymerization in Monolayers and Ultrathin Films

Jie Ji[‡,1], Yao Li[‡,1], Sven Bernaerts[2], Kunal S. Mali[2], Rui Ding[1], Hongzhen Lin[3], Louis Cuccia,[4] Steven De Feyter[2], Oleksandr Ivasenko*[1], Lifeng Chi*[1] and Yuan Fang*[1]*

[1] State Key Laboratory of Bioinspired Interfacial Materials Science, Institute of Functional Nano & Soft Materials (FUNSOM), Soochow University, Suzhou 215123, Jiangsu, PR China

[2] Division of Molecular Imaging and Photonics, Department of Chemistry, KU Leuven,

Celestijnenlaan 200 F, 3001 Leuven, Belgium.

[3] i-Lab, Suzhou Institute of Nano-Tech and Nano-Bionics, Chinese Academy of Sciences, Suzhou 215123, Jiangsu, PR China.

[4] Department of Chemistry and Biochemistry, Concordia University, Montreal, Quebec H4B 1R6, Canada.

Table of contents:

Experimental Section

Chemicals and Materials. 10,12-pentacosadiynoic acid (PCDA), 10,12-heptacosadiynoic acid (DA-27) (both 99% purity, Shanghai Aladdin), tetradecane (98%, Shanghai Aladdin) and chloroform (99%, Chinasun Specialty Products Co.) were used without further purification. Toluene (98.5%, Shanghai Aladdin) was distilled before use.

Preparation of monolayer film.

1) Langmuir-Blodgett (LB) film

PCDA was dissolved in chloroform (2×10^{-3} M) and spread on Milli-Q in an LB trough (KSV 5000). The surface pressure was adjusted to 15 mN/m and held constant during deposition onto freshly cleaved highly oriented pyrolytic graphite (HOPG) substrates *via* vertical dipping at a lifting speed of 1 mm/min.

2) Tilted drop-casting

Freshly cleaved HOPG substrates were tilted at a 30° angle, and 7–8 drops of a 1×10^{-4} M PCDA-toluene solution were drop-cast at a rate of 0.5 seconds per drop. The substrate was then dried by blowing nitrogen gas across the surface.

3) Spin-coating

A 1×10^{-4} M PCDA-toluene solution was spin-coated onto freshly cleaved HOPG at 8000–10000 rpm under ambient conditions to form a molecular layer.

4) Optimized drop-casting with time for self-assembly/equilibration

Several droplets of the 5×10^{-5} M PCDA-toluene solution were drop-cast onto a freshly cleaved horizontally positioned HOPG surface, forming a bulging liquid droplet. As the droplet size slightly diminished, additional drops were added. After 4 minutes, the liquid was quickly removed by blowing nitrogen gas, leaving a monolayer PCDA dry film.

5) Monolayers at the liquid-solid interface

4 μL of DA-27 1×10^{-3} M in tetradecane was drop-cast on freshly cleaved HOPG, followed by STM characterization.

Preparation of multilayered thin film. A thin film of PCDA on a quartz plate was prepared by drop-casting of 80 μL of a 5.9×10^{-2} M of PCDA chloroform solution. The film was further dried with nitrogen blowing.

Polymerization of diacetylene films. Polymerization in controlled atmosphere can be easily carried out using very simple set-ups (Figure S13b), but the most convenient and precise method for us was the use of the environmental cell in the Cypher VRS (Figure S13a). The latter allowed not only to control the temperature during the annealing step (optimally for our study: 50 minutes at 50°C followed by 10 minutes, all carried out under a stream of N_2 (15-20 mL/min) to remove residual toluene and minimize solvent-induced defects, this step ensured a clean HOPG baseline), but also the flow of gas atmosphere during polymerization. After annealing, the nitrogen flow rate was maintained at 15–20 mL/min for an additional 10 minutes

to prevent ambient air ingress. As the system cools from 50°C to room temperature, the air inside the enclosed cell contracts, potentially allowing oxygen to enter. To mitigate this, we maintained nitrogen purging to ensure a stable inert atmosphere. While a high flow rate is not strictly required at this stage, it serves as a precautionary measure to prevent air ingress during cooling. We found (Figure S14) that to obtain high-quality polymerization film (*e.g.*, Figure 3d in the main text), it was best to have a slow stream of nitrogen (0-5 mL/min, this optimized flow rate minimizes the turbulence while maintaining an oxygen-free environment, which enhanced polymerization efficiency) during polymerization. For the photopolymerization, a hand-held UV lamp (YGSEH-UVC-5 Compact, 5 W, 254 nm) was positioned 1 cm above the surface, with a power density of 5 mW/cm^2 (measured using a digital UV-C meter, ZDZ-1). Variations in irradiation times resulted in different polymerization yields. For larger 2×2 cm^2 quartz plates, a UV lamp with a bigger spot size (UVGO, 12 W, 254 nm) was positioned 2 cm above the surface, with a power density was 2.5 mW/cm^2.

Quantification of Polymer Yield by qNMR. Polymer yield was quantified using terephthalaldehyde as an internal standard for NMR. ^{1}H NMR spectra were obtained, and the integrated signals of PCDA protons were normalized against the internal standard. This allowed the determination of the absolute molecular weight of PDA.

Spectroscopic Characterization. UV-VIS absorption spectra of UV-irradiated PCDA films on quartz plates were measured using a UV-VIS-NIR spectrophotometer (PE750, PerkinElmer, USA). FT-IR transmission spectra of UV-irradiated PCDA films on KBr windows were recorded using a VERTEX 70v spectrometer (400–3000 cm^{-1}). Raman spectra were collected on a Horiba LabRam HR800 spectrometer using a 633 nm laser, with 5–10 accumulations of 10–60 s scans (0–3400 cm^{-1}).

Microscopic Characterization. Atomic force microscopy (AFM) was performed in tapping mode (Cypher VRS) using Multi75Al-G probes (resonance frequency: ~75 kHz, spring constant: ~3 N/m), with image analysis *via* WSxM5.0 software.[1] Scan rates were maintained at 1–3 Hz with a resolution of 512 × 512 pixels. To minimize tip-related artifacts, we carefully removed organic contamination from AFM probes using controlled UV/O_3 treatment (UVO Cleaner, Jelight Company) for a short duration, ensuring no significant alteration of tip properties. Probes were replaced if degradation or contamination was detected, and tip sharpness was routinely verified using a reference substrate (freshly cleaved HOPG). Scanning tunneling microscopy (STM) was conducted in constant current mode (Cypher VRS) with Pt/Ir probes, with analysis using WSxM5.0. Imaging parameters include tunneling current (I_{set}) and sample bias voltage (V_{bias}). Scanning electron microscopy (SEM) was performed using a Hitachi SEM at 15 kV to observe the distribution of thin films.

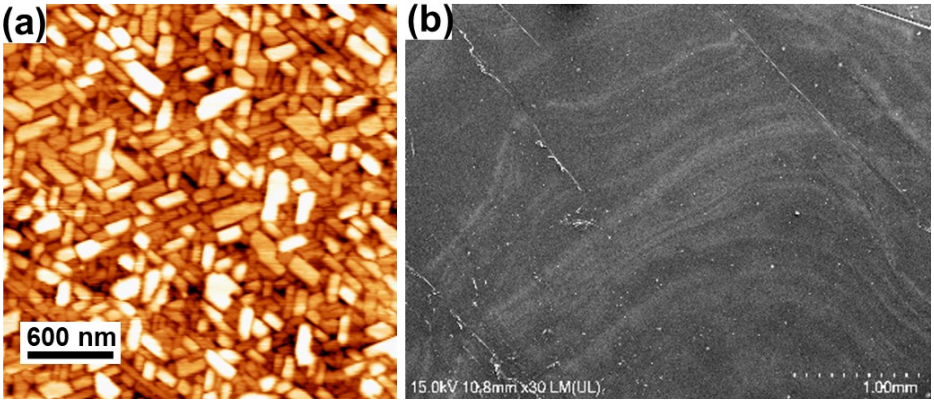

Figure S1. PCDA self-assembled film prepared simply by placing a small drop (<3 μL) of PCDA solution in toluene over HOPG results in quick uncontrolled drying yielding multilayered thin film with variable thickness: (a) AFM image of PCDA multilayer film; (b) large-scale SEM image of PCDA film showing clear "coffee rings".

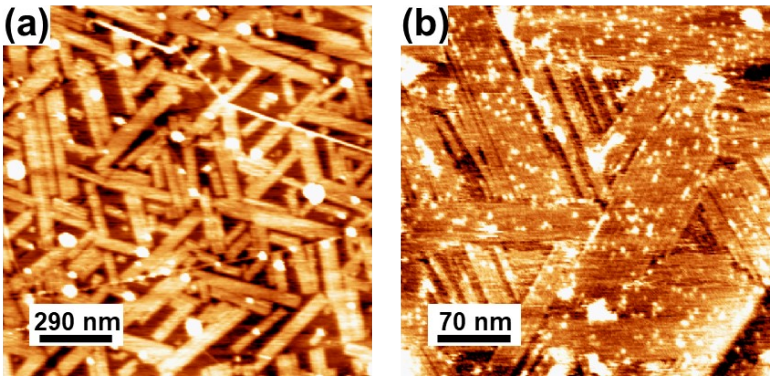

Figure S2. PCDA self-assembled film prepared with unpurified toluene as solvent before and after polymerization. Nanoparticles of impurities hinder reliable characterization of polymerized chains. (a) PCDA self-assembled film prepared using unpurified toluene as solvent. There are many white spots. (b) Polymerization of PCDA films prepared with unpurified toluene. After polymerization, a large number of small white dots appear on the polymer chain, and these white dots could be mistaken for polymers.

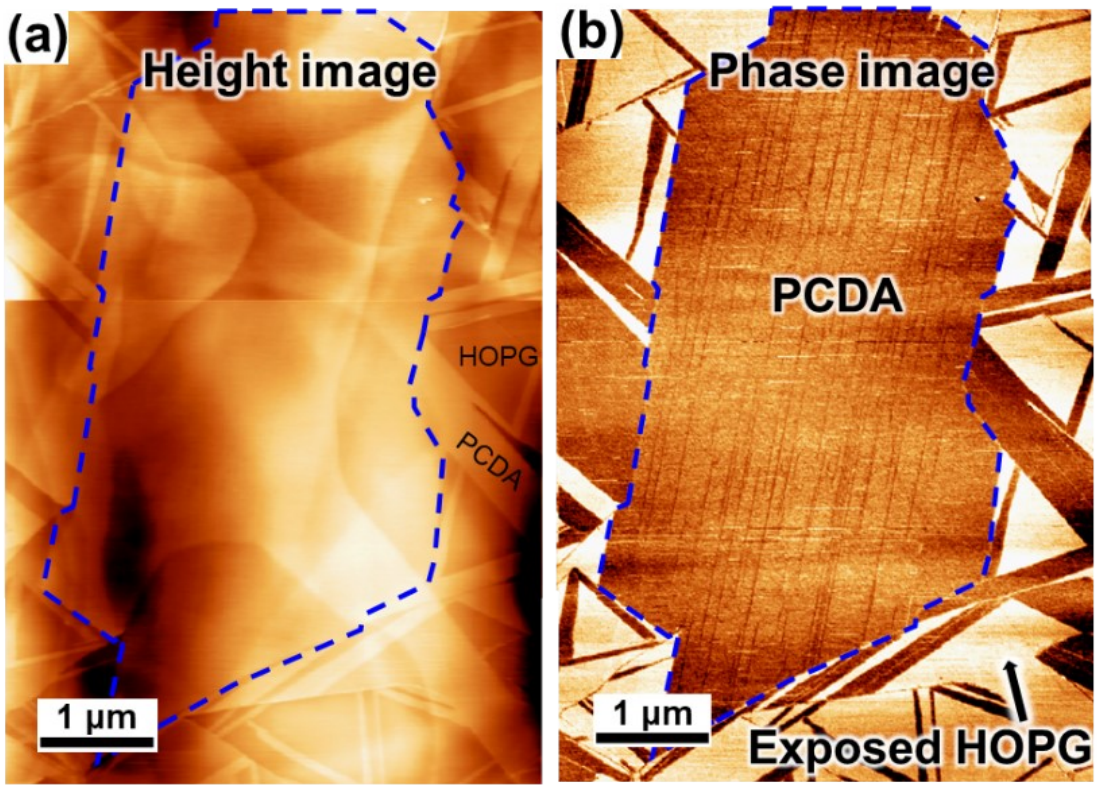

Figure S3. An example of AFM images of large PCDA domains that can be prepared by drop-casting with a short equilibration time. This sample was used in photopolymerization studies and so is partially polymerized: dark polymer lines can be seen in the phase image.

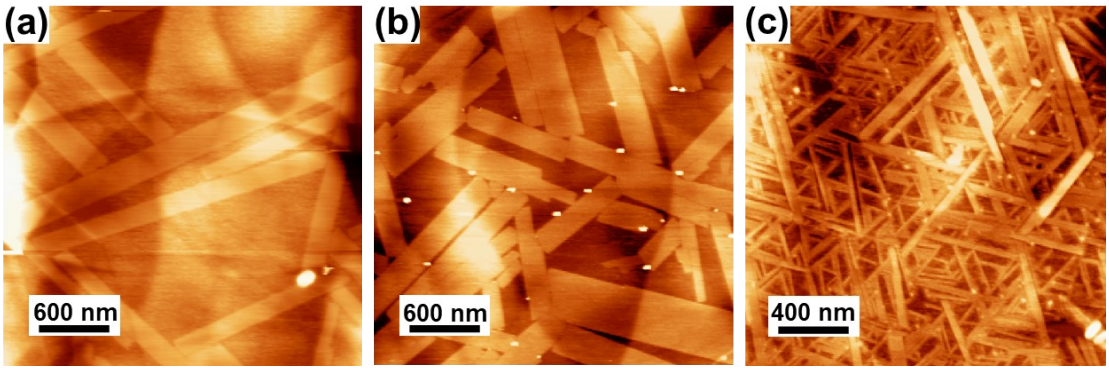

Figure S4. AFM height images of PCDA monolayers prepared by varying the concentrations of the drop-casted solutions. The PCDA monomer molecules were dissolved in toluene at a concentration of (a) 1×10^{-5} M, (b) 5×10^{-5} M, (c) 2×10^{-4} M.

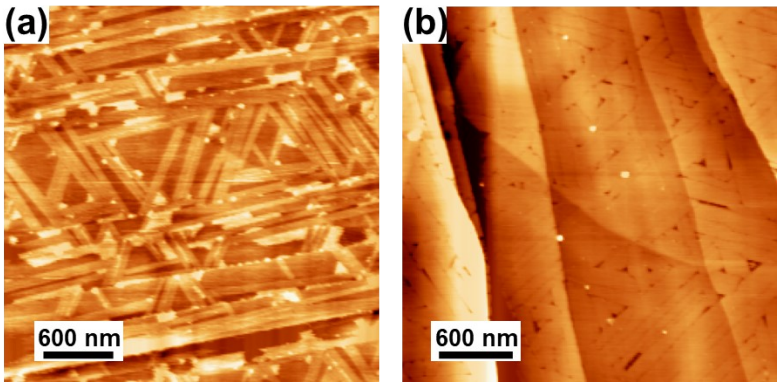

Figure S5. AFM height images of PCDA self-assembled film prepared by modified perpendicular drop-casting method at room temperature (a) and after heating for 61℃ (b, c). Large scale image (b) illustrates the growth of domains and improved uniformity of the monolayer, while small scale image (c) shows proofs of the beginning of thermal polymerization at temperatures above 60℃.

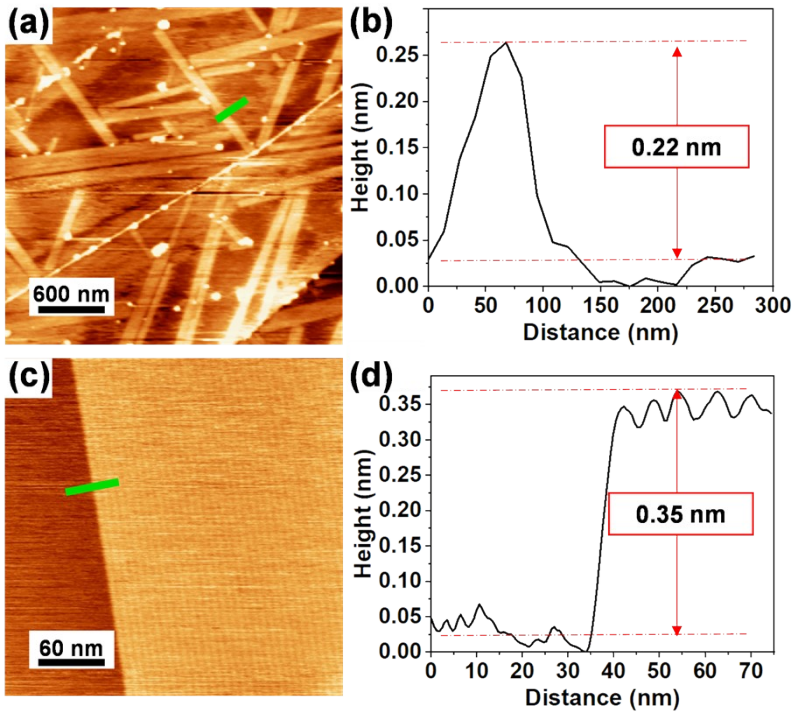

Figure S6. The influence of residual solvent and water traces on the height measurements of PCDA film. (a-b) PCDA self-assembled film before annealing. Height measurement is not accurate. (c-d) PCDA self-assembly after ~50℃ annealing. The traces of solvents are removed, and the height measurements are reproducible and correct. A part of image (c) was used in Figure 2c.

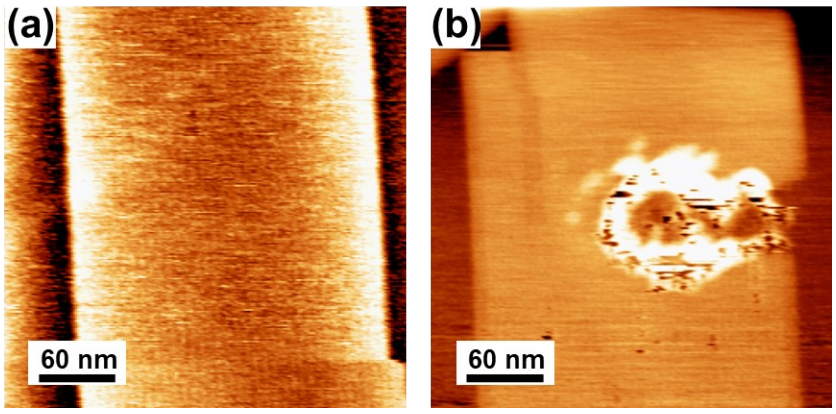

Figure S7. AFM height images of PCDA self-assembled film before (a) and after (b) "nanowriting". The nanowriting caused small molecules to accumulate into a small mound.

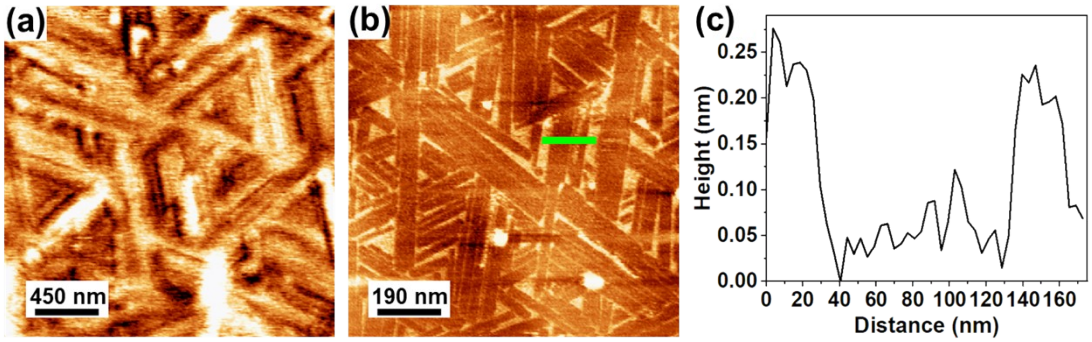

Figure S8. AFM height images of PCDA self-assembled film scanned by using degraded (a) or contaminated tips (b) can compromise resolution, appearance (observed inverted contrast in (b)) and height measurement accuracy (c).

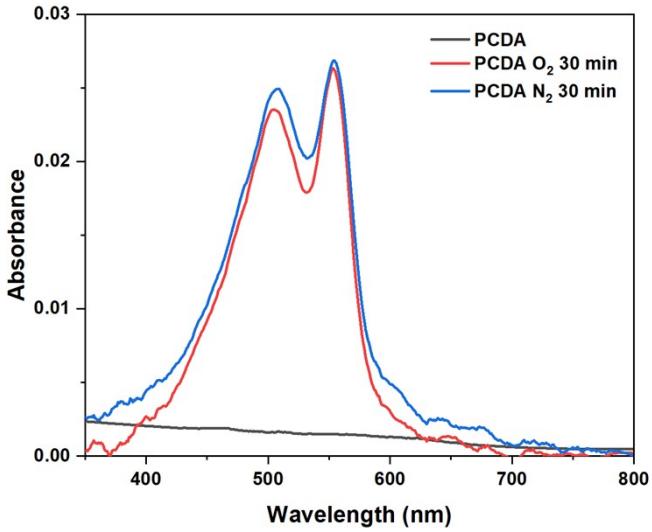

Figure S9. UV-vis spectra of PCDA film on quartz glass. The UV absorption peaks of the PCDA film after polymerization under nitrogen and under air are of the same height, which may be caused by the inconsistency of the film thickness.

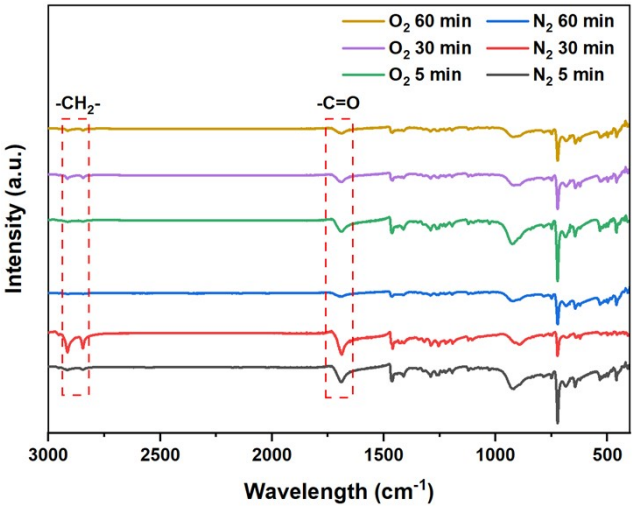

Figure S10. FT-IR spectra of PCDA films polymerized under air and nitrogen for different times (5 min, 30 min, 60 min) on KBr substrate. Peaks below 1500 cm^{-1} belong to fingerprint region. Peaks in 2915, 2847 cm^{-1} are $-CH_2-$, peak in 1691 cm^{-1} is C=O in COO^{-1}. Differences in C=O intensity are due to the different film thickness.

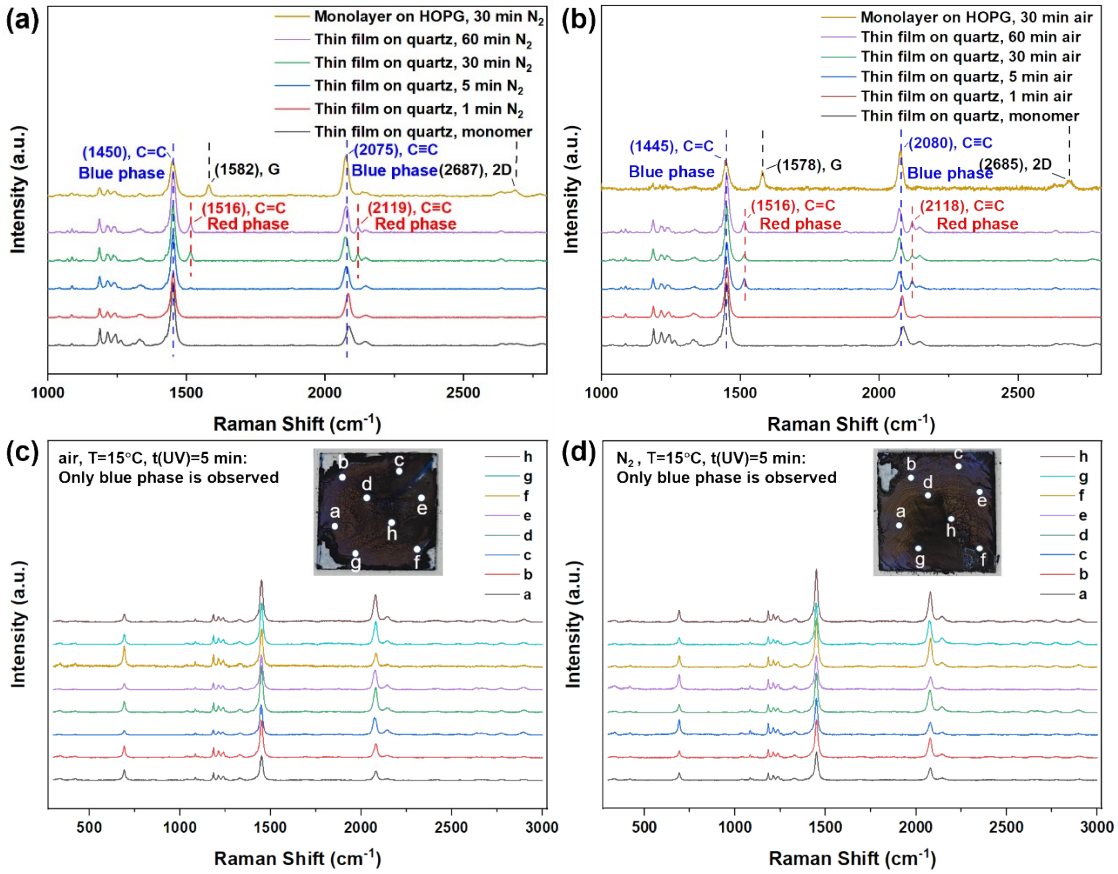

Figure S11. (a, b) Raman spectra of PCDA thick films on quartz glass and PCDA monolayer films on HOPG, polymerized for different durations under air were analyzed. The Raman spectra of PCDA before polymerization on the HOPG surface show only the G-peak band at around 1578 cm^{-1} and the 2D-peak band at around 2685 cm^{-1} for HOPG, as well as the C≡C characteristic peak at around 2244 cm^{-1} for PCDA. After polymerization, the bands at around 1445 cm^{-1} are attributed to the C=C stretching modes of the polymer backbone. Raman spectrum of PCDA polymerized in nitrogen and air atmosphere both have blue phase and red phase polymer signals. In nitrogen, red phase showed up at a later polymerization time, presumably because nitrogen flow provided additional cooling to the samples, slowing down local heating and thus preventing the blue-to-red phase transition. (c, d) Our control experiments shown that conducting polymerization at the surrounding temperature ≤15°C allows easy formation of blue phase poly-PCDA both in nitrogen and in air.

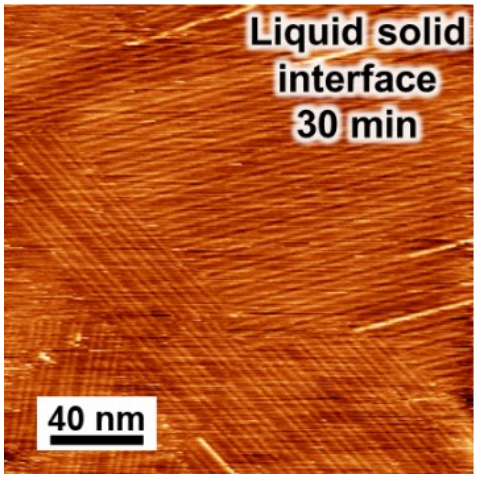

Figure S12. High-resolution STM image of the polymerized 10,12-Heptacosadiynoic acid (DA-27) film under air for 30 min at the n-tetradecane/HOPG interface (V_{bias} = -0.6 V, I_{set} = 10 pA). The polymer chain is short and the polymerization yield is low. The reason for choosing DA-27 here is that the alkyl chain of PCDA is short and weakly adsorbed onto the surface and could be easily interrupted by UV illumination, inducing desorption during polymerization.

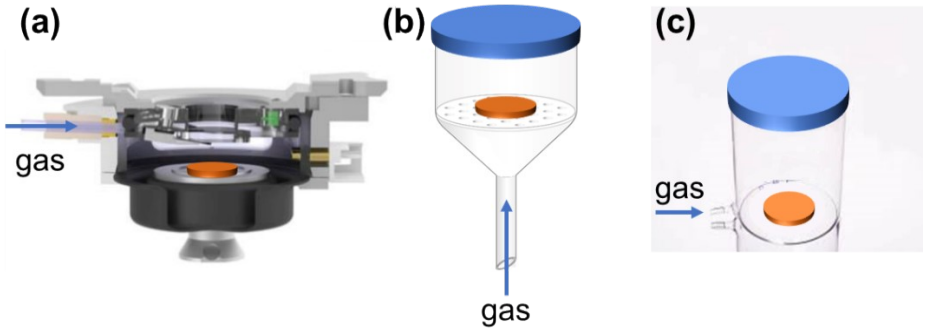

Figure S13. Different setups used for N_2 purging during polymerization. (a) Air perfusion cell. (b) Büchner funnel. (c) Bottom-armed beaker. The geometry and purging velocity of each setup influence the polymerization outcome. We observed that high nitrogen flow rate (15-20 mL/min) during polymerization leads to the formation of many bright small spots in AFM images (Figure S14a,b). To achieve high-quality polymer monolayers, it is crucial to avoid directly blowing nitrogen onto the sample, as in configuration (c). Instead, a low, stable nitrogen flow (<5 mL/min) should be maintained to minimize turbulence while effectively excluding oxygen.

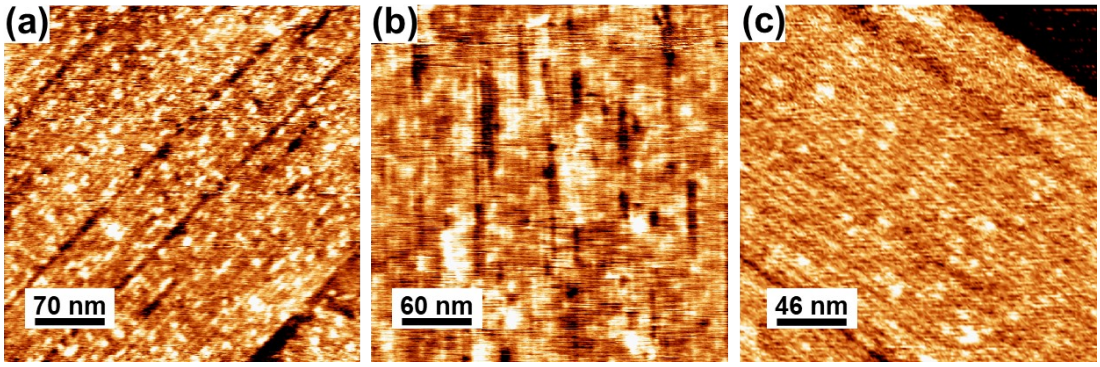

Figure S14. AFM images of PCDA self-assembled films polymerized under different blowing rate of nitrogen, (a) before and (b) after toluene solvent purification polymerized for 60 min at blowing speed of 15-20 mL/min, (c) before toluene solvent purification polymerized for 5 min at blowing speed of 0-5 mL/min. The AFM image of PCDA self-assembled film after toluene solvent purification polymerized for 5 min at blowing speed of 0-5 mL/min can be found in figure 3d. The blowing speed is the nitrogen flow rate on Cypher VRS. We observed that a higher nitrogen flow rate (15–20 mL/min) during polymerization led to the appearance of small bright spots (~0.5 nm) in AFM images. While the exact origin of these features is still under investigation, possible contributing factors include rearrangement of loosely bound polymer fragments, localized surface contamination, or subtle monolayer perturbations induced by high gas flow. To minimize these artifacts, we found that a low, stable nitrogen flow (0–5 mL/min) provided the best polymerization results by balancing oxygen exclusion with minimal disturbance to the monolayer.

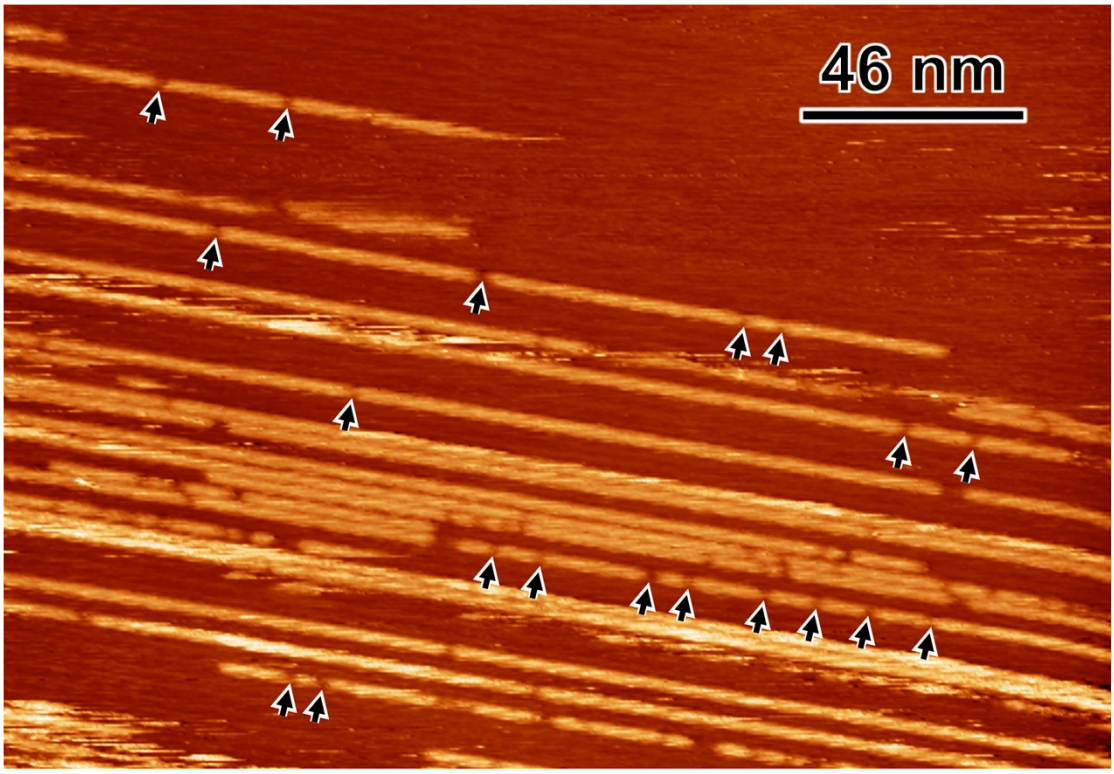

Figure S15. Pronounced 1D nano-alignment of polymers as resolved in STM image of dry annealed PCDA monolayers that were polymerized in air. Imaging parameters: V_{bias} = -0.6 V, I_{set} = 10 pA.

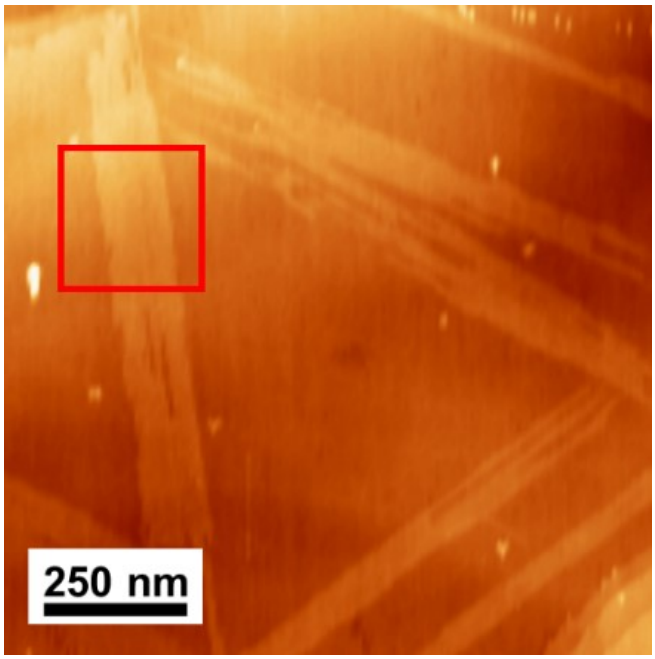

Figure S16. AFM images of polymerized PCDA self-assembled film before nanowriting. The area in the red box is the area where the AFM image of PDA in Figure 2 (c).

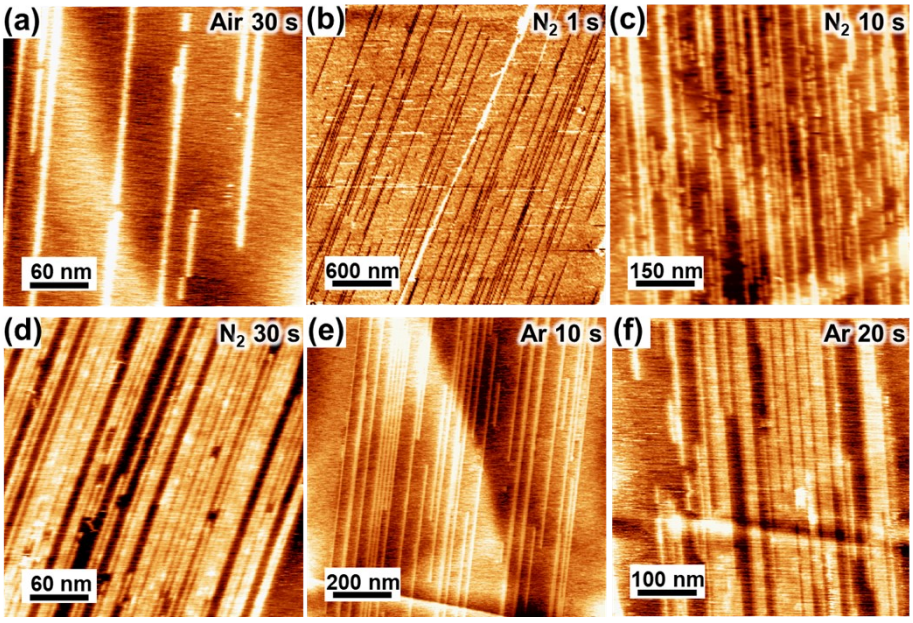

Figure S17. AFM images of PCDA self-assembled film for every exposure condition. (a) Under air for 30 s, (b) under N_2 for 1 s, (c) under N_2 for 10 s, (d) under N_2 for 30 s, (e) under Ar for 10 s, (f) under Ar for 20 s. Except for the phase image in (b), all other others are topography images.

Table S1. Polymerization efficiency and polymer number density quantified in AFM images of partially polymerized PCDA/HOPG samples at indicated polymerization times. 'Adjusted' values for polymerization efficiency were very roughly approximated by multiplying the number of counted polymer chains that were longer than certain threshold polymerization degree (240 for N_2 and argon, 150 for air). Even with so rough adjustments, the polymerization efficiency is somewhat lower than reported[2] under UHV environment.

	Air 5 min	**Air 30 s**	**N_2 30 s**	**N_2 10 s**	**N_2 1 s**	**Ar 10 s**	**Ar 20 s**	**Air 30 min (Liquid-solid surface)**
Dose (mJ/cm^2)	1500	150	150	50	5	50	100	9000
Polymer number density ($nm^{-2} \times 10^3$)	0.2381	0.0444	0.8018	0.4667	0.0074	0.0757	0.4367	0.0002
	0.1703	0.0682	0.6301	0.6556	0.0058	0.0660	0.3309	0.0005
	0.1776	0.0363	0.7313	0.3987	0.0054	0.0636	0.3066	0.0005
	0.2330	0.0667	0.7342	0.3690	0.0094	0.0687	0.2646	
	0.2330	0.0611		0.1520	0.0051	0.0829	0.3060	
	0.1667	0.0357		0.2922	0.0073	0.1026	0.3095	
	0.1620	0.1000		0.1470	0.0070	0.1411	0.3342	
	0.1889			0.1865		0.1181		
Mean	0.1960	0.0589	0.7244	0.3335	0.0068	0.0898	0.3269	0.0004
STDEV	0.0329	0.0227	0.0613	0.1651	0.0015	0.0281	0.0495	0.0001
α	1.3×10^{10} Adjusted: 2.2×10^{10}		5.0×10^{11} Adjusted: 2.7×10^{12}			3.0×10^{11} Adjusted: 1.7×10^{12}		4.4×10^{6}

Section S1. The derivation of polymerization efficiency as a function of polymer number density and UV dose.

Following Prof. Takajo's derivation[2] it can be shown that: the polymer generation rate is

$$\frac{d\sigma}{dt} = \frac{k_\alpha \alpha M_0}{\alpha'}$$

where α and α′ are the rate constants of the photoexcitation and decay of radicals, M_0 is the monomer density, σ is the polymer number density, and k_α is the rate constant of the addition reaction. With the UV dose defined by

$$D = It$$

where I is the intensity of the UV light, the rate constant of photoexcitation can be written as $\alpha = cI$, where c is a constant. Then, the polymer generation efficiency

$$\beta = \frac{d\sigma}{dD} = \frac{ck_\alpha M_0}{\alpha'}$$

The rate constants for radical decay in air and nitrogen can be denoted as α'_{air} and α'_{N2}, respectively. Assuming that quenching by oxygen and nitrogen are independent processes, that are linearly proportional to the quantities of the quenching molecules (~21% O2 and ~79% of inert gases), we can write: $\alpha'_{air} = 0.79\ \alpha'_{N2} + 0.21\ \alpha'_{O2}$. Then, we can see that the major contribution to high quenching efficiency comes from oxygen ($\alpha'_{N2} / \alpha'_{N2} > 180$).

When identifying quenching efficiency of oxygen, nitrogen and n-tetradecane molecules in the experiments with photopolymerization at the liquid-solid interface, we have taken known[3] Ostwald coefficient of air in n-dodecane (0.18).

$$C(air) = \frac{RT}{LP} = \frac{0.18 * 1}{0.0821 * 298} = 0.0074\ (M)$$

Where: *C* is the solubility in (mol/L), *L* is the Ostwald coefficient, *P* is the partial pressure of the gas (in atmospheres), *R* is the universal gas constant, approximately 0.0821 $L \cdot atm \cdot K^{-1} \cdot mol^{-1}$, *T* is the temperature in Kelvin. Then according to partial pressures, the concentrations of oxygen and inert gases are $1.5 \cdot 10^{-3}$ M and $5.8 \cdot 10^{-3}$ M, respectively, and cannot explain the observed low quenching efficiency in liquid n-tetradecane. For these experiments we have also used DA-27 (Figure S12), which forms more stable adlayers and is even less prone to desorption of its polymers into liquid phase than DA-25. A possible explanation of the observed quenching is the result of significantly increased frequency and interaction time between photoexcited diacetylene and molecules of the media, due to >500x larger density (0.762 g/ml vs. $1.293 \cdot 10^{-3}$ g/ml) and >100 times greater viscosity of n-tetradecane compared to air (2.13 mPa·s vs. 0.0185 mPa·s).[4]

Section S2. Quantification of polymer length distribution

The polydispersity index (PDI), number-average (DP_n) and weight-average (DP_w) degrees of polymerization can be useful when comparing polymers prepared by different ways. represent important the average number of repeating units per polymer chain, calculated by:

$$DP_n = \frac{M_n}{M_0}; \quad DP_n = \frac{M_w}{M_0}; \text{ PDI} = \frac{M_w}{M_n}$$

Where: M_n is the number-average molecular weight, determined by dividing the total mass of all polymer molecules by the total number of polymer molecules, M_w is the weight-average molecular weight, and M_0 is the molar mass of the repeating unit (monomer M_0(PCDA)=374.69 g/mol). The estimated DP_n, DP_w and DPI for the annealed PCDA assemblies that were later polymerized in air, nitrogen and argon were:

	all samples were annealed before polymerization in:		
polymer property	**air**	**nitrogen**	**argon**
DP_n	175	2121*	2306*
DP_w	221	4074*	3622*
PDI	1.27	1.92*	1.57*

*These values are probably overestimated if only few of the registered "extra-long" polymers are individual chains. Considering the P(N) distribution shape, we believe more reasonable values of the DP_n and DP_w of the produced poly-PCDA in inert gases are in the range 400-600.

Section S3. Quantification of polymer yield in thick (~10 μm) films by qNMR

To guarantee the maximum reliability of the quantification, terephthalaldehyde (99%, Shanghai Macklin) was used as the internal standard for NMR. Importantly, the signal from the standard does not overlap with the signals from our materials and thus, it can be easily integrated.

As a first step, it was verified that the signals of the internal standard do not overlap with those of the analyte. The solubility and compatibility of the substances was also verified, checking that the sample, the analyte and the solvent did not react. This was verified by comparing a ^{1}H NMR of the samples at t = 0 and t = 24 h.

Polymer of PCDA induced by UV irradiation is insoluble in chloroform which is verified by ^{1}H and ^{13}C NMR. To determine the polymer yield, samples made by the procedure described above were scraped off, carefully weighted, and dissolved in a known mass of deuterated chloroform with a known amount of internal standard. Finally, an ^{1}H NMR spectrum was measured, and the signals from the nonlabile carbon-bound protons of PCDA were integrated and normalized using the signal from the internal standard. As the integrated peak of each signal is directly proportional to the number of protons, these results allowed us to determine the absolute mass of PCDA.

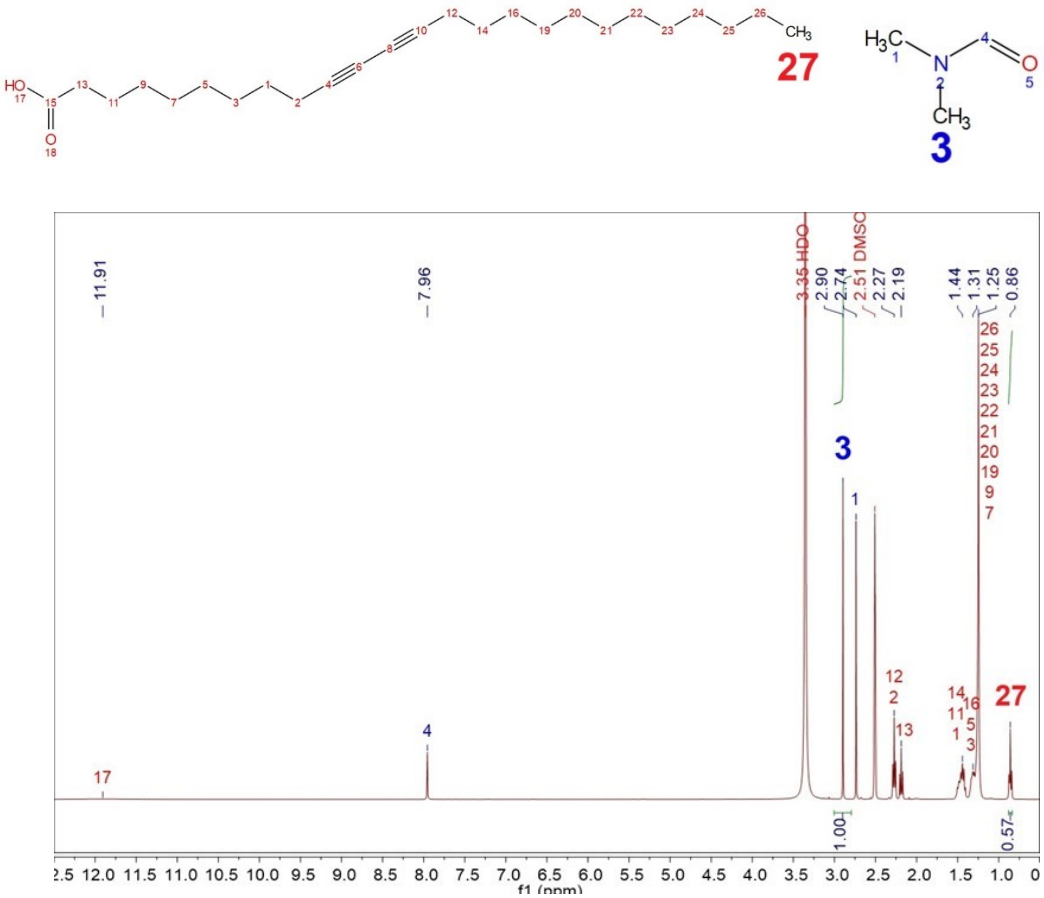

Sample (mg):	(4.78 ± 0.01)
DMF (wt%):	(0.164 ± 0.001)
Deuterated reagent (mg):	(905.36 ± 0.01)
Calculated polymer yield (%):	(9 ± 3)

Figure S18. ^{1}H NMR (DMSO-d6) of PCDA film after polymerization for 1 min in N_2 environment.

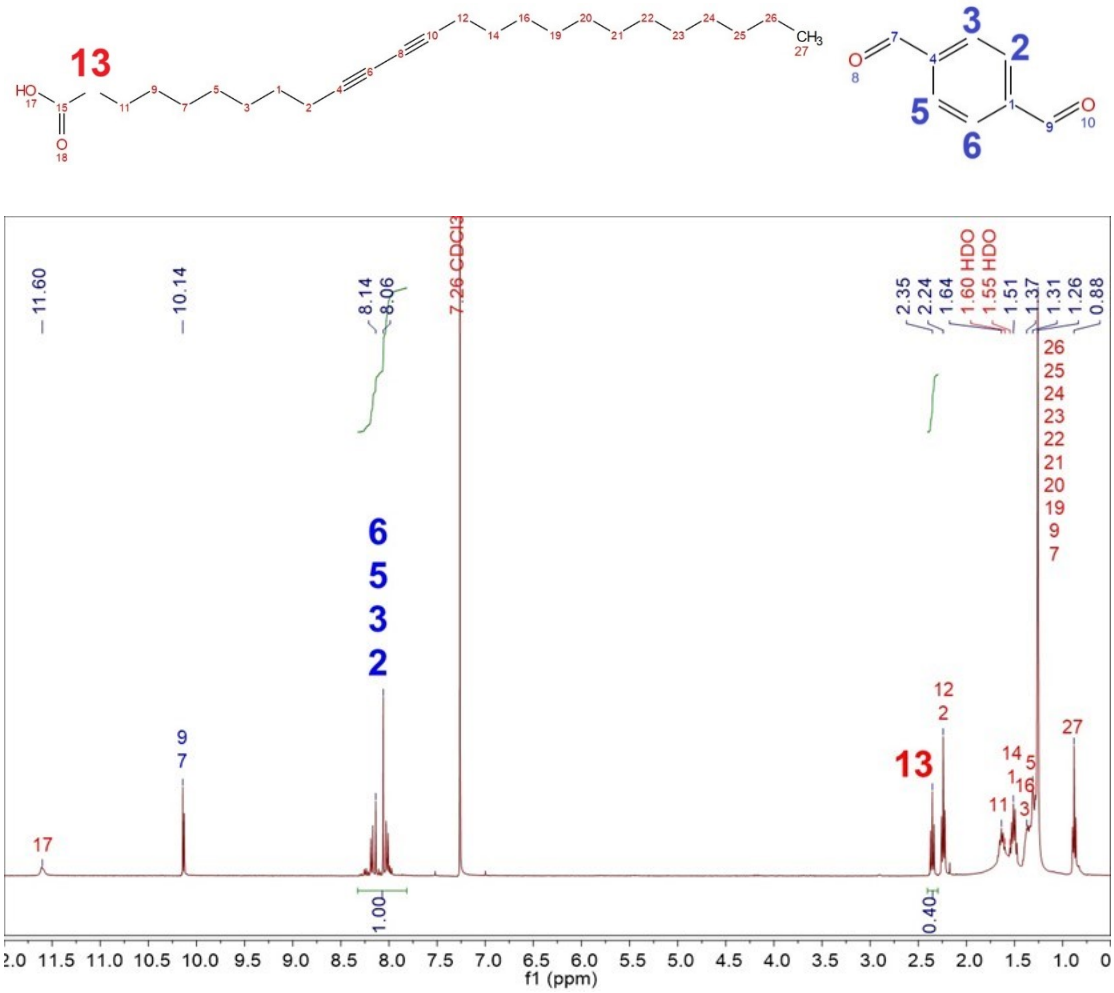

Sample (mg):	(2.26 ± 0.01)
TA (wt%):	(0.0539 ± 0.0001)
Deuterated reagent (mg):	(1099.89 ± 0.01)
Calculated polymer yield (%):	(41 ± 3)

Figure S19. ^{1}H NMR ($CDCl_3$) of PCDA film after polymerization for 5 min in N_2 environment.

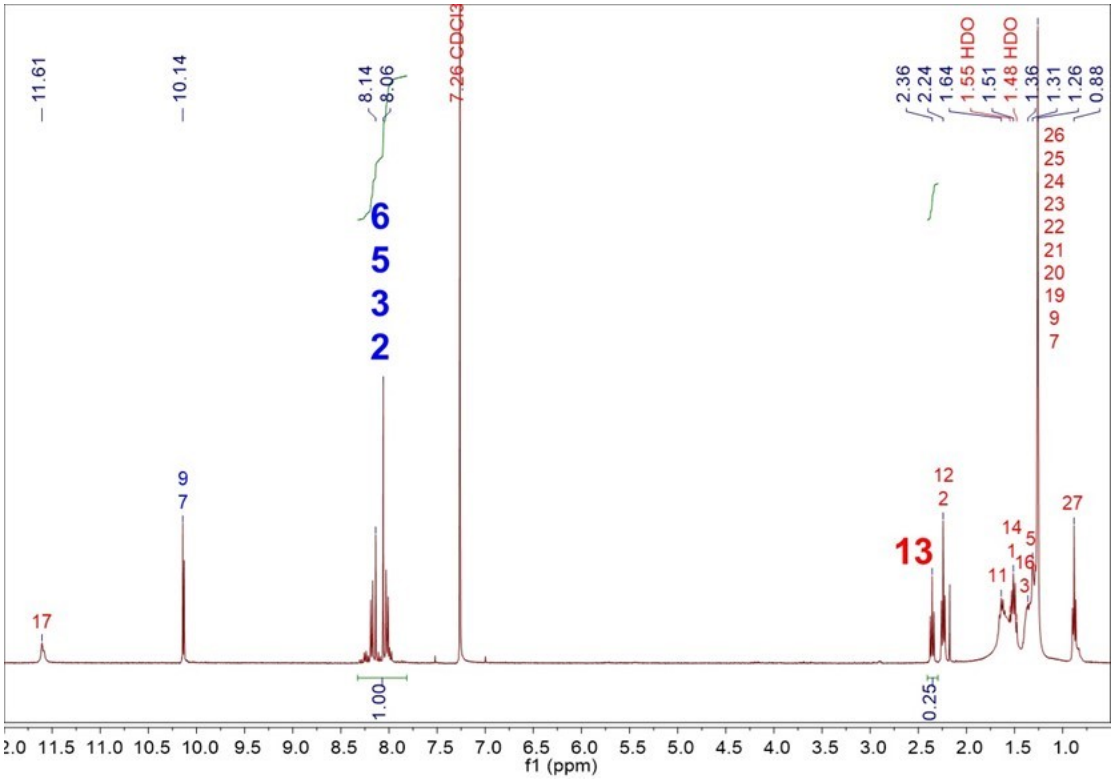

Sample (mg):	(2.88 ± 0.01)
TA (wt%):	(0.0539 ± 0.0001)
Deuterated reagent (mg):	(875.31 ± 0.01)
Calculated polymer yield (%):	(77 ± 1)

Figure S20. ^{1}H NMR ($CDCl_3$) of PCDA film after polymerization for 30 min in N_2 environment.

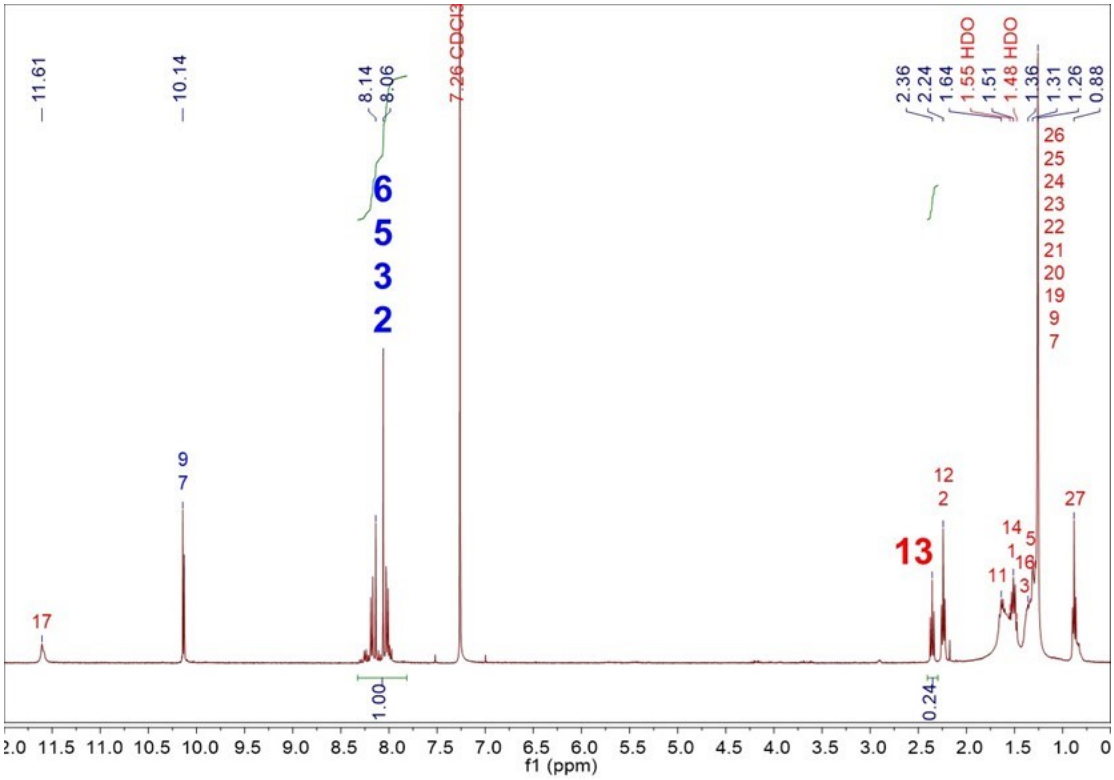

Sample (mg):	(2.96 ± 0.01)
TA (wt%):	(0.0539 ± 0.0001)
Deuterated reagent (mg):	(896.51 ± 0.01)
Calculated polymer yield (%):	(78 ± 1)

Figure S21. ^{1}H NMR ($CDCl_3$) of PCDA film after polymerization for 60 min in N_2 environment.

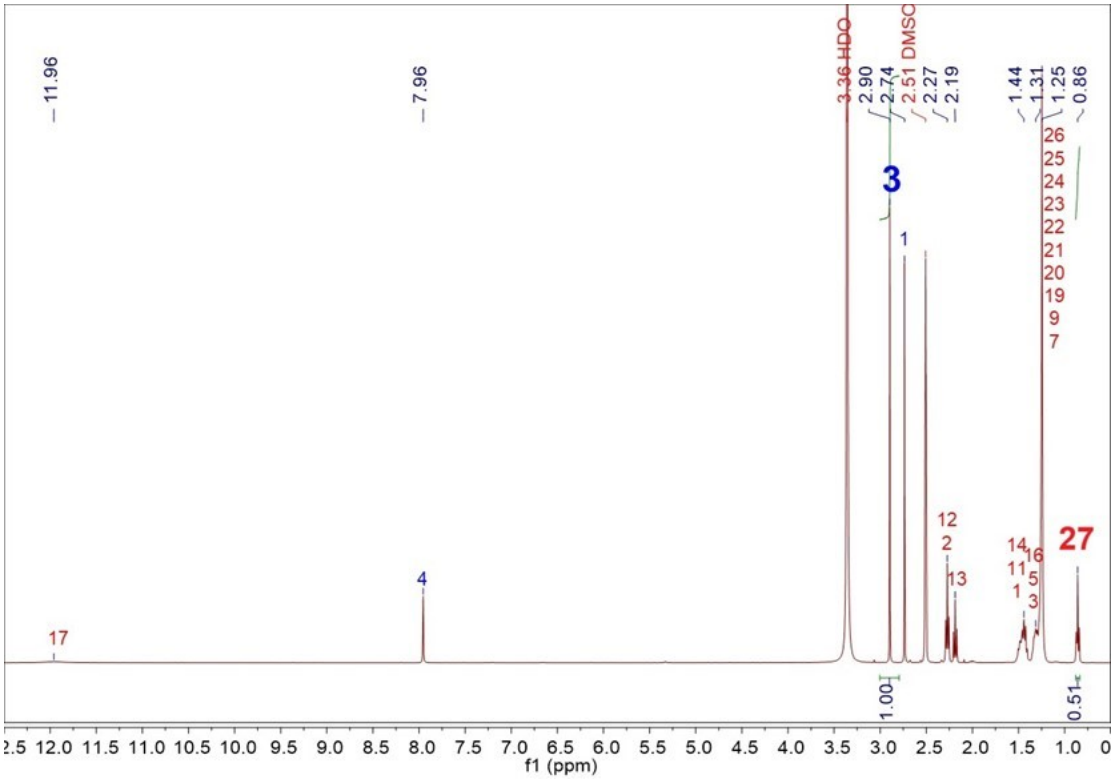

Sample (mg):	(3.82 ± 0.01)
DMF (wt%):	(0.164 ± 0.001)
Deuterated reagent (mg):	(905.33 ± 0.01)
Calculated polymer yield (%):	(-2 ± 4)

Figure S22. ^{1}H NMR (DMSO-d6) of PCDA film after polymerization for 1 min in O_2 environment.

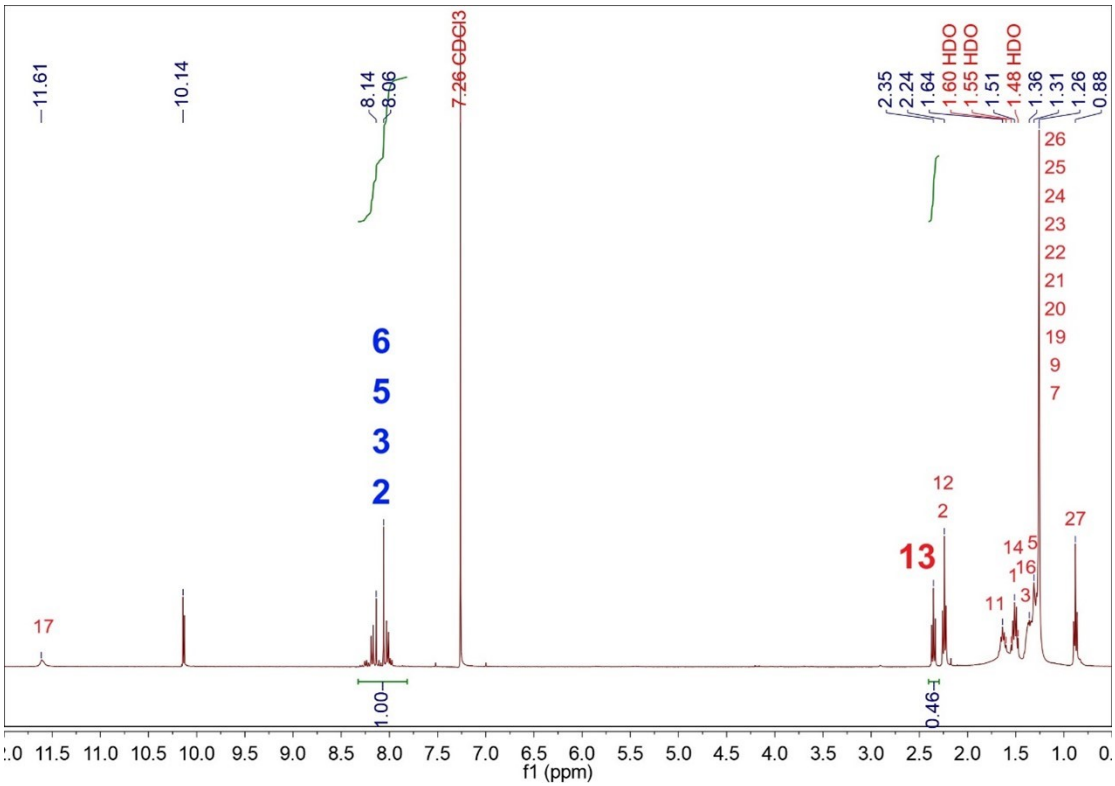

Sample (mg):	(2.38 ± 0.01)
TA (wt%):	(0.0539 ± 0.0001)
Deuterated reagent (mg):	(1036.74 ± 0.01)
Calculated polymer yield (%):	(40 ± 3)

Figure S23. ^{1}H NMR ($CDCl_3$) of PCDA film after polymerization for 5 min in O_2 environment.

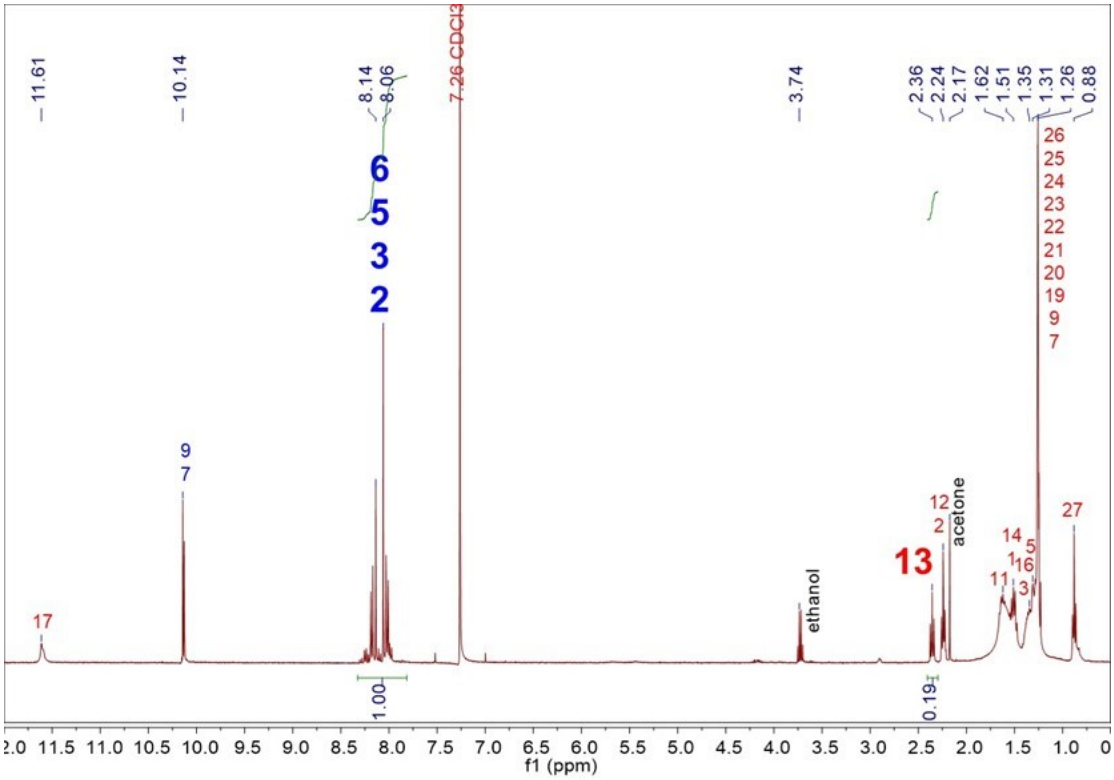

Sample (mg):	(2.45 ± 0.01)
TA (wt%):	(0.0539 ± 0.0001)
Deuterated reagent (mg):	(1163.86 ± 0.01)
Calculated polymer yield (%):	(71 ± 2)

Figure S24. ^{1}H NMR ($CDCl_3$) of PCDA film after polymerization for 30 min in O_2 environment.

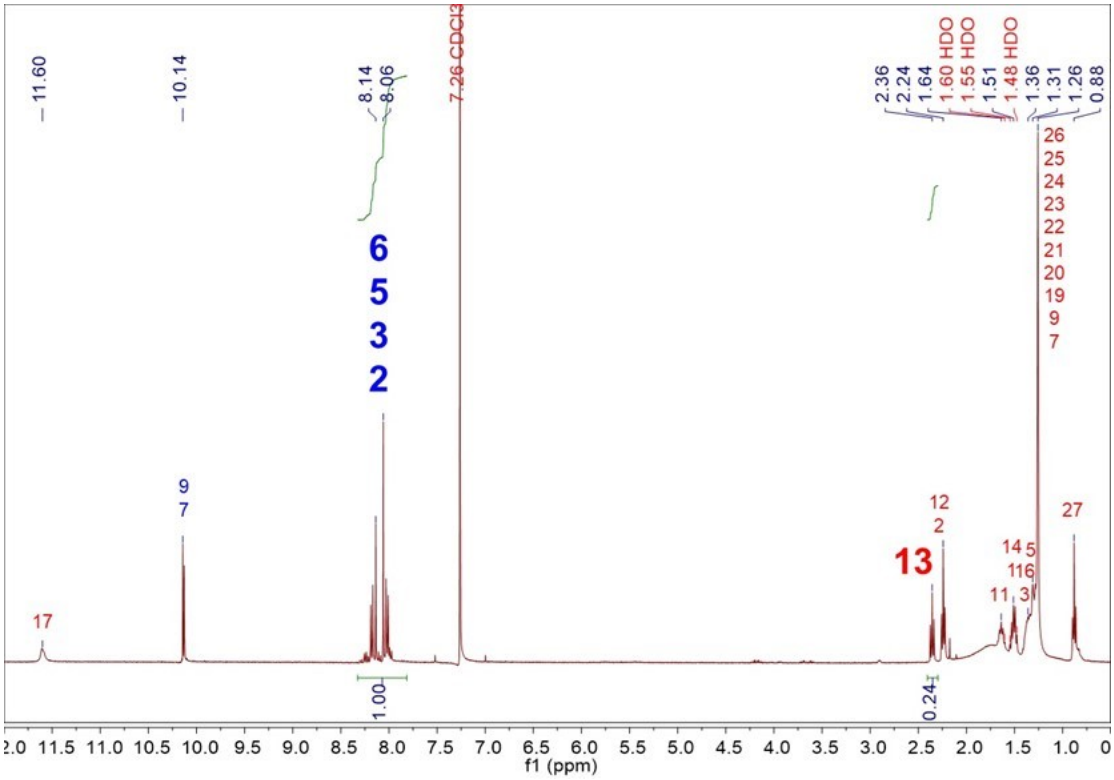

Sample (mg):	(3.79 ± 0.01)
TA (wt%):	(0.0539 ± 0.0001)
Deuterated reagent (mg):	(1006.50 ± 0.01)
Calculated polymer yield (%):	(81 ± 1)

Figure S25. ^{1}H NMR ($CDCl_3$) of PCDA film after polymerization for 60 min in O_2 environment.

References:

1. I. Horcas, R. Fernández, J. M. Gómez-Rodríguez, J. Colchero, J. Gómez-Herrero and A. M. Baro, *Rev Sci Instrum.*, 2007, **78**, 013705.
2. D. Takajo and K. Sudoh, *Langmuir*, 2021, **37**, 6002-6006.
3. R. Battino, T. R. Rettich and T. Tominaga, *J. Phys. Chem. Ref. Data*, 1984, **13**, 563-600.
4. National Center for Biotechnology Information. PubChem Compound Summary for CID 12389, Tetradecane. https://pubchem.ncbi.nlm.nih.gov/compound/Tetradecane. Accessed Mar. 18, 2025